Supplementary Information

The *in-situ* redispersion of PdCu alloy catalyst under the $CFCl_2CF_2Cl$ atmosphere: a combination of experimental and DFT study

Haodong Tang[1]*, MingMing Dang[1], Feiran Zhang[2], Bin Xu[1], Lichun Li[1], Weiyu Song[2], Wenfeng Han[3], Ying Li[3] and Zongjian Liu[1]*

[1]*College of Chemical Engineering, Zhejiang University of Technology, 18 Chaowang Road, Hangzhou 310014, PR China.*

[2]*State Key Laboratory of Heavy Oil Processing, China University of Petroleum (Beijing), Beijing, P.R. China*

[3]*Industrial Institute of Catalysis, Zhejiang University of Technology, Hangzhou 310032, PR China.*

*Corresponding author –Dr Haodong Tang, tanghd@zjut.edu.cn; Dr Zongjian Liu, zjliu@zjut.edu.cn

1. Experimental

Chemicals

$CFCl_2CF_2Cl$ (99.5%) gas was obtained from Zhejiang Research Institute of Chemical Industry; Active carbon was purchased from Hang Zhou Wan Jing New Material Co., Ltd; AR grade HCl solution was obtained from Shanghai Hongguang Chemical Factory; $Cu(NO_3)\cdot 3H_2O$ (99.8%) was obtained from Shanghai Macklin Biochemical Technology Co., Ltd; $PdCl_2$ (99.98%) was purchased from Sino-Platinum Metals Co., Ltd. N_2(99.999%), H_2 (99.999%) were purchased from Hangzhou Minxing Industry and Trade Gas Co., Ltd.

Preparation of Sintered Catalysts, metal/AC-S

The active carbon supported PdCu bimetallic and monometallic (Pd, Cu) catalysts were prepared by impregnation method. The Pd content was sourced from a mixed 0.05 M $HCl/PdCl_2$ solution and Cu content sourced from 0.05 M $Cu(NO_3)_2$ solution. Before the impregnation, available activated carbon was dried overnight at 373 K. After that, the corresponding metal salt solutions were added onto the active carbon support and treated by ultrasonic for 20 minutes at 298 K. The mixture was then aged for 12 h at room temperature to ensure the successful impregnation. The resulting sample was subsequently dried overnight at 383K to remove the excess amount of water. The dried sample was then loaded to a fixed bed reactor and subjected to a reduction process. The sample was heated up to 575K (10 K/min) and flushed with H_2 (20 ml/min) for three hours. In order to simulate the deactivation of catalysts via thermodynamic sintering, the fresh catalysts were further calcined at 673 K for 2 hours under pure N_2 flow of 40 mL/min. And then the catalysts were cooled to room temperature under the same atmosphere. The resulting catalysts were labelled as sintered catalysts, metal/AC-S. Same method was used to prepare the monometallic Pd/AC and Cu/AC catalysts.

Redispersing of sintered catalysts, metal/AC-R

To perform the catalysts redispersion process, the sintered catalysts were treated with a mixture gas of 0.06 mL/min $CFCl_2CF_2Cl$ and 20mL/min H_2 at 573 K for 30 h and then the catalystswere cooled at inert gas N_2 atmosphere (40 mL/min).The resulting catalysts were marked as redispersed catalysts, metal/AC-R.

Characterization

The X-ray powder diffraction (XRD) characterization was recorded on a Rigaku instrument equipped with scintillation counter detector by using nickel-filtered CuKα (0.15418 nm) radiation source over the range of $30\ ° \leq \theta \leq 90\ °$. We have used

High resolution transmission electron microscopy (HRTEM) has been executed using a JOEL JEM-1200EX microscope with a field emission gun as source of electrons. The point-to-point resolution of the microscope was 0.20 nm operated at 160 kV. Samples were deposited on Molybdenum (Mo) or Nickel (Ni) grid by placing a few droplets of a suspension of ground sample in ethanol on the grid, followed by drying at ambient conditions.

X-ray photoelectron spectroscopy (XPS) using an ESCALAB210 instrument (Physical Electronics) equipped with an Mg target Kα X-ray radiation source (hυ =

1253.6 eV). The binding energy (BE) scale was calibrated using a C 1s peak at 284.60 eV.

Computational details

All calculations were performed with the density functional theory (DFT) as implemented in the Vienna Ab Initio Simulation Package [1, 2].The projector augmented wave (PAW) method was used to describe the interactions between the ions and the electrons with frozen-core approximation [3, 4]. The Perdew-Burke-Ernzerhof (PBE) electron exchange-correlation functional was adopted as well [5]. PAW potentials acted on the self-consistently optimized 4d electrons of Pd, 3d/4s electrons of Cu, 3s/3p electrons of Cl, 2s/2p electrons of F, and 2s/2p electrons of C. Kinetic cut-off energy was set in 400 eV. Γ-point-centered Monkhorst−Pack k-point meshes of 3×3×1 were used for the Brillouim zone integration. The stable point was identified by the conjugate gradient method until the forces acting on each ion were smaller than 0.05 eV/Å. The energy criterion for convergence of the electron density was set at 10^{-4} eV. Transition state was calculated by climbing image nudged elastic band method (CINEB) [6].

The bulk equilibrium lattice constants of Cu are a = b = c = 3.614 Å and α=β=γ= 90°. Because Pd is evenly dispersed on the surface of Cu, $PdCu_3$ model was built by replacing one Cu atom with one Pd atom on the primitive cell of Pd to to keep the ratio of Pd:Cu to be 1: 3. Next the 111 surface was cleaved based on the $PdCu_3$ alloy model. Then (2×2) supercell for the $PdCu_3$ surface was built. Different Pd(111) has been investigated in previous study [7]. The adsorption and dissociation of $CClF_2$-CCl_2F was investigated on the most stable (111) surface of Pd and Cu_3Pd. The two top atomic layers of the (111) surface of Pd and Cu_3Pd were allowed to relax and the rest of two atomic layers were fixed. The vacuum gap thickness was set to 15 Å. The adsorption energy is defined as following：

$$E_{ads}=E_{adsorbate+surface}-E_{adsorbate}-E_{surface} \quad (1)$$

in which, $E_{adsorbate+surface}$ is the total energy of the adsorbate interacting with the slab, and E(adsorbate) and E(substrate) are the energies of free adsorbate in gas phase and bare surface, respectively. Therefore, a negative value corresponds to an exothermic adsorption, and a more negative value shows a stronger adsorption.

2. CO oxidation reaction

Carbon monoxide oxidation was chosen as probe reaction to examine the catalytic performance of sintered and redispersed catalysts. About 0.5 g of the catalyst was placed in the tubular flow reactor where the mixed gas flow containing reactant O_2 (20 mL/min), CO (10 mL/min) and N_2 (170mL/min) passing through. The reaction was performed at 120 °C under atmosphere condition. The composition of the gas phase was determined by a gas chromatography (GC9560) equipped with TCD analyser. The catalytic activity of the three different forms of the bimetallic PdCu/AC catalysts, including the fresh, sintered and redispersed forms are shown in Figure S2. Under same reaction conditions, the CO conversion is 65.8% over the fresh PdCu/AC catalyst. After calcination of the catalyst under N_2 at 673 K, the CO conversion rate over PdCu/AC-S catalyst drops dramatically to ~17%. After the R-113/H_2 gas treatment, the CO conversation rate restored to same level as the fresh catalyst. This proves that the redispersion of Pd to small particles can recover the catalytic performance to the same level as that of the fresh catalyst.

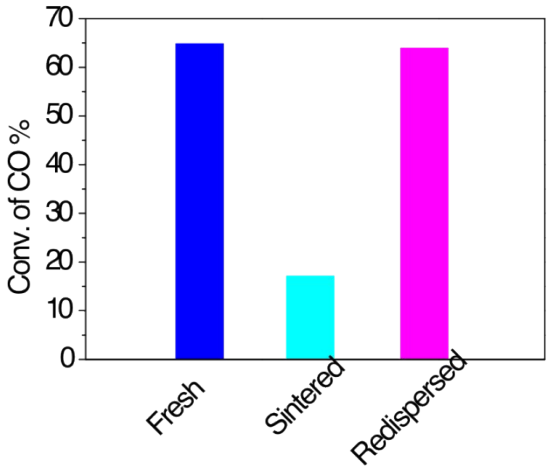

Figure S1. Conversion rate of CO oxidation over 3 bimetallic PdCu/AC catalysts including PdCu/AC-F (Fresh)、PdCu/AC-S (sintered)、PdCu/AC-R (redispersed)

3. Redispersion of Cu/AC catalyst

The same R113/H_2 gas treatment was applied for monometallic Cu/AC-S catalyst as well to explore the effectiveness of the dispersion process on monometallic Cu/AC-S catalyst. The XRD patterns of the sintered and redispersed Cu/AC catalysts are shown in Figure S2.

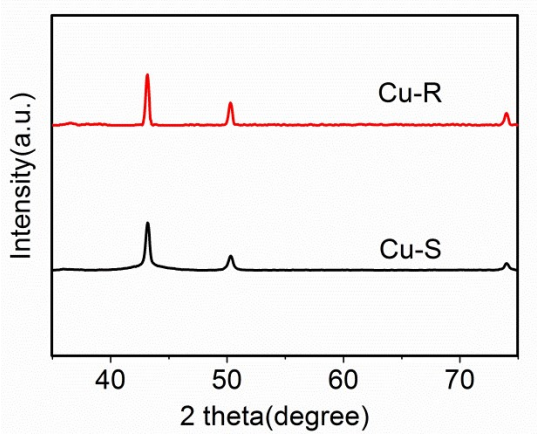

Figure S2. XRD patterns of the Cu/AC-S and Cu/AC-R catalyst

As can be seen from Figure S1, there are no obvious changes can be observed between the XRD patterns of the sintered and redispersed Cu/AC catalysts, indicating no noticeable redispersion of the Cu/AC-R catalyst. This was also confirmed with the estimated Cu crystal size with 21.4 nm and 26.2 nm before and after the R113/H_2 gas treatment. According to the standard reducing potential of Cu (0.3419 eV) and Pd(0.951 eV), Cu is more active and supposed to go through the interaction with R-113 and form oxidized Cu species (Cu^{2+}) on the surface of the alloyed catalysts. However, due to the low sintering/Tammann temperature (678 ^{o}C), the aggregation process totally dominates and suppresses the redispersion process of the single Cu metal.

4. **Two-step redispersion process**

A two-step redispersion process**,** namely firstly treated by R113 and then reduced by H_2, was also tested for the redispersion of the sintered PdCu/AC catalyst. The sintered catalyst was firstly treated with R113 at 300 ^{o}C for 5 hours and then reduced by H_2 for 2 hours at the same temperature. The TEM images of the redispersed PdCu/AC-R' are shown in Figure S3. According to Figure S3, the crystal size of the PdCu/AC-R' catalyst reduced to about 11 nm after the step by step oxidation-reduction process. This confirm that treat with R113 at evaluated temperatures, the formation of oxidative intermediates occurs and initiates the redispersion process.

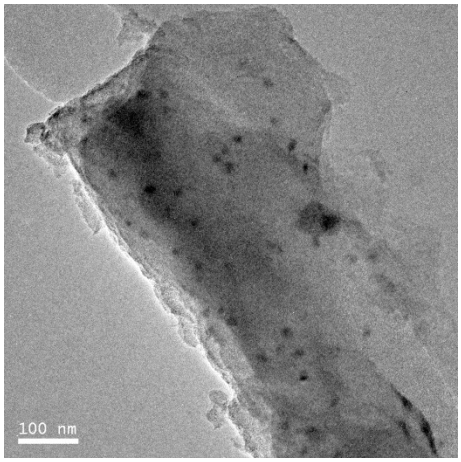

Figure S3. TEM image of the PdCu/AC-R' catalyst

5、XPS Spectra

The Cl 2p XPS spectra of the PdCu/AC catalyst before and after the R113/H_2 gas treatment was presented in Figure S4. The peak at binding energy of 197.8 and 200.7 eV were assigned to Pd-Cl and Cu-Cl bond while the peak at binding energy of 200.2 eV was assigned to the present of organic chlorine on the surface of the catalyst. It is clear that the content of Pd-Cl bond increases significantly after the R113/H_2 gas treatment, indicating the presence of PdCuClx intermediate on the surface of the PdCu/AC catalyst.

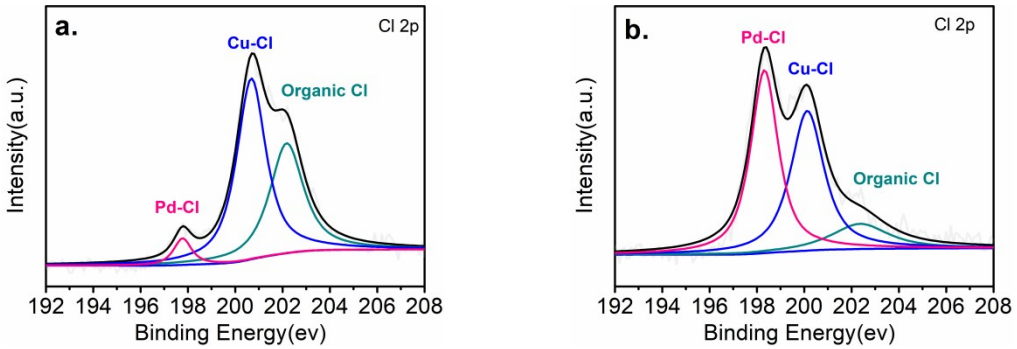

Figure S4. The XPS spectra of Cl 2p region obtained for catalysts of PdCu/AC-S (a) and PdCu/AC-R (b).

References

1. Kresse G, Hafner J, *Phys. Rev. B:* Condens. Matter, 1994, **49**, 14251-14269.
2. G. Kresse, J. Hafner, *Phys. Rev. B*, 1993, **47**, 558-561.
3. P. E. Blöchl, *Phys. Rev. B*, 1994, **50**, 17953-17979.
4. G. Kresse, Joubert D, *Phys. Rev. B*, 1999, **59**, 1758-1775.
5. J. P. Perdew, *Phys. Rev. Lett.*, 1996, **77**, 3865.
6. Z. Duan, G. Henkelman, *ACS Catal.*, 2014, **4**, 3435-3443.

7. X. Nie, X. Jiang, H. Wang, W. Luo, M. J. Janik, Y. Chen, X. Guo and C. Song, *ACS Catal.*, 2018, **8**, 4873-4892.